UNIZIK JOURNAL OF ENGINEERING AND APPLIED SCIENCES (UJEAS)

Research Article

Corrosion inhibition of mild-steel in sulphuric acid solution using expired Promethazine - Theoclate drug as inhibitor

Linda Nnodi, Ifeanyi John Obibuenyi, Ikechukwu A. Nnanwube, Okechukwu D. Onukwuli, Monday Omotioma

Special Issue

A Themed Issue in Honour of Professor Onukwuli Okechukwu Dominic (FAS).

This special issue is dedicated to Professor Onukwuli Okechukwu Dominic (FAS), marking his retirement and celebrating a remarkable career. His legacy of exemplary scholarship, mentorship, and commitment to advancing knowledge is commemorated in this collection of works.

Edited by
Chinonso Hubert Achebe PhD.
Christian Emeka Okafor PhD.

UJEAS

UNIZIK JOURNAL OF ENGINEERING AND APPLIED SCIENCES

UNIZIK Journal of Engineering and Applied Sciences 4(1), March (2025), 1658-1673
Journal homepage: https://journals.unizik.edu.ng/index.php/ujeas
PRINT ISSN: 2992-4383 || ONLINE ISSN: 2992-4391

Corrosion inhibition of mild-steel in sulphuric acid solution using expired Promethazine -Theoclate drug as inhibitor

Linda Nnodi[1], Ifeanyi John Obibuenyi[2], Ikechukwu A. Nnanwube[2]*, Okechukwu D. Onukwuli[3], Monday Omotioma[4]

[1]Chemical Engineering Department, Chukwuemeka Odumegwu Ojukwu University, Uli Campus, Anambra State, Nigeria.
[2]Chemical Engineering Department, Madonna University Nigeria, Akpugo Campus, Enugu State, Nigeria.
[3]Chemical Engineering Department, Nnamdi Azikiwe University, PMB 5025, Awka, Anambra State, Nigeria.
[4]Chemical Engineering Department, Enugu State University of Science and Technology, P.M.B. 01660, Enugu, Nigeria.
*Corresponding Author's E-mail: ik.nnanwube@gmail.com

Abstract
The purpose of this study is to investigate the effectiveness of expired promethazine-theoclate in sulphuric acid environment as mild-steel corrosion inhibitor. The drug was characterized for its functional groups and chemical constituents using infrared spectroscopy and gas chromatography methods. Experimental techniques and gravimetric methods were also employed. The inhibitory effects (thermodynamic and adsorption parameters) of the drug were assessed. Inhibition efficiencies were optimized and modeled using RSM and ANN models. The predominant functional groups were found to be O-H, CO-NH-CO stretches; =C-H stretching; N-H deformation, and contains 2, 4- di-tert-butylphenol, 1-Heptadecene, tridecane, Propyl 11-octadecenoate, and others. The heat of adsorption (Q_{ads}) results at various inhibitor concentrations were all negative with a value of -67151.6 J/mol with promethazine-theoclate concentration of 0.8 g/L. The Frumkin isotherm provided the best fit from the isotherm fittings since it gave the highest average R^2. Gibb's free energy of adsorption values of -10.23 kJ/mol and -10.29 kJ/mol at 313 K and 323 K, respectively, indicated that promethazine-theoclate molecules' adsorption was physical and not chemisorption. Maximum efficiency of 92.89% was attained from the gravimetric method. The ANN gave better prediction of inhibition efficiency with higher value of R^2 (0.9999) and lower values of RMSE (0.0180) and SEP (0.0230). RSM optimization gave an optimum efficiency of 92.39 %. The impedance method displayed a capacitive loop, signifying charge-transfer process, and polarization measurements indicated that the drug was a mixed-type inhibitor. Hence, promethazine-theoclate proved to be an excellent inhibitor for controlling mild steel corrosion in H_2SO_4 media.
Keywords: Corrosion control, Mild steel, Sulphuric acid, Expired drug, Inhibitor

1. Introduction

Steel is a versatile engineering material that is broadly deployed in various applications owing to its excellent ductility, toughness, high machinability, and weldability. A large portion of the steel produced is utilized in chemical industrial sectors to handle salt, acid, and alkali solutions. Although mild-steel has added to the challenge of dealing with corrosion, its continuous use and popularity as an engineering material is not only based on its good mechanical properties but also on good economic advantages because of its relative accessibility and affordability. Thus, preserving the functionality of these metallic structures and increasing their service life depend heavily on the corrosion protection of metallic substrates. Acid solutions used in industries cause severe corrosion of metallic structures (Omotioma and Onukwuli, 2019; Udeh et al., 2021).

Corrosion is simply the degradation of a substance caused by an inevitable reaction with the environment. A metal that interacts with its surroundings and sustains damage due to accidental chemical or electrochemical attacks is said to have undergone corrosion. It causes metal loss through the breakdown and loss of properties, which puts equipment safety at risk. For the fact that corrosion requires the maintenance and replacement of metallic structures that break prematurely, it is a significant economic loss. More focus is placed on prevention and control as a more workable and realistic approach to minimizing the impact of corrosion damage because there are numerous factors that contribute to corrosion. These include the nature of metals, their variability in the environment, and their applications. This ensures that corrosion is inevitable, making it difficult to eliminate. Inhibitors are substances introduced to corrosive environments to alter the reaction between the environment and metal surface, thereby preventing or reducing corrosion. Corrosion inhibitors control or prevent corrosion via various mechanisms (Omotioma et al., (2024(a, b); Onukwuli and Omotioma, 2019**)**.

The application of inhibitors is the most practical and dependable method to prevent corrosion under acidic and aqueous conditions. There has been a significant rise in the usage of pharmaceutical drugs as corrosion inhibitors. Owing to the fact that most drugs are synthetic forms of organic chemicals, they are environmentally-friendly. In acidic solutions, several medications, including irbesartan, ampicillin, chloramphenicol, tramadol, and sodium diclofenac salt, have been utilized as corrosion inhibitors. Consequently, expired medications should be used to profit from drug waste. The approach addresses both economic and environmental issues since it converts drug wastes to raw materials with the potential of protecting the environment from the toxic effects of drug waste. Therefore, the wide application of hydrochloric acid, potassium hydroxide etc., and metals such as carbon steel and aluminum have given the need for the present study to investigate the actions of expired promethazine-theoclate in sulphuric acid as corrosion inhibitor of mild-steel. However, the inability of the mild steel to form a passive layer renders it vulnerable to corrosive attacks **(**Umoren et al., 2021; Omotioma et al., 2019**)**.

Over time, it has been demonstrated that the most effective method to prevent corrosion of mild steel and aluminum is the use of corrosion inhibitors. However, the use of organic and inorganic chemical corrosion inhibitors is restricted owing to high cost of their synthesis, reduced biodegradability, toxicity, and environmental hazards. Therefore, it is necessary to identify appropriate substitutes to conventional inhibitors by the usage of pharmaceutical drugs that have expired. Utilizing expired medications could solve two additional delicate issues: lowering drug-related environmental pollution and reducing drug disposal expenses. The majority of expired medications contain amines, and some also have functional groups in their molecular structures such as sulfide, sulfoxide, or sulfonamide. These compounds are known to possess corrosion inhibitory properties (Onukwuli et al., 2025).

Available studies have not investigated the actions of expired promethazine-theoclate drugs in acidic environments. Previous studies have explored various drugs such as pyrazinamide, isoniazid, rifampicin, atenolol, sulfamethoxazole and norfloxacin for use as mild-steel corrosion inhibitors, but the efficacy of expired promethazine-theoclate drug remains unexplored. Hence, promethazine-theoclate was utilized in this study to mitigate mild-steel corrosion in sulphuric acid (H_2SO_4) solution under various operating conditions. This study aims to fill this gap by conducting experiments to evaluate the corrosion inhibition capabilities of this drug. Hence, the study provides new insights into corrosion science and pharmaceutical applications through systematic experiments and analyses with techniques such as gravimetric (weight loss), electrochemical (impedance spectroscopy and polarization measurements), and surface studies.

2.0 Materials and methods

2.1 Materials

2.1.1 Mild Steel and inhibitor

Mild-steel used is composed of S (0.12 %), Cr (0.02 %), C (0.24 %), Mn (0.13 %), Ni (0.07 %), P (0.22 %), Si (0.05 %), and Fe (99.15 %). The drug used is expired promethazine-theoclate.

2.1.2 Preparation of H_2SO_4 solution and concentrated promethazine-theoclate

1 M H_2SO_4 solution was prepared analytically using distilled water. Analytical grade acid was used. Distilled water (700 ml) and 54.35 ml of H_2SO_4 were mixed in one-liter measuring cylinder and more distilled water was added to make up the solution to one liter. Different concentrations of expired drug were prepared. In each flask, 10 g of the drug was added to make a solution of sulphuric acid. From these, inhibitor solution samples were prepared at concentrations of 0.2 - 1.0 g/L from the solution stock. Preliminary investigation was conducted to determine the best concentrations of expired promethazine-theoclate to be used for this study.

2.1.3 Mild Steel Preparation

The 3 x 3 cm mild-steel specimens were cut into coupons. To obtain a shiny, polished surface, coupons were washed to remove grease by applying acetone, it was then cleaned with distilled water, dried naturally, and placed in desiccators to eliminate any oil and organic contaminants remaining. The initial weights of the coupons were recorded. Thereafter, they were labeled to ensure seamless identification.

2.2 Methods

2.2.1 Characterization of expired drug, promethazine-theoclate

Chemical analysis of the drug was performed. The combined features of mass spectrometry (MS) and gas chromatography (GC) were applied to identify various substances within the drug sample. When heated, the drug split into distinct substances which were allowed to pass through a column filled with nitrogen to identify the compounds. The GC-MS model used is the GC-MS 5977B and 7890A MSD. The detailed operating conditions had been reported (Onukwuli et al., 2024a).

2.2.2 Functional groups of the inhibitor

High spectral resolution data over a broad range were simultaneously collected using spectrophotometer. The raw data were transformed into an actual spectrum using Fourier transform infrared (FTIR). Analyses of the different FTIR-produced peaks were conducted to identify the proper functional groups**.** Metals were submerged in the medium while the inhibitor was present to obtain the corrosion products. The corrosion products were gathered in beakers. The FTIR model deployed for the analysis was Cary 630. The detailed procedure had been reported (Onukwuli et al., 2024a).

2.2.3 Weight loss method

2.2.3.1 Weight loss based on one-factor-at-a-time (OFAT)

The weight loss technique is a reliable method of measuring corrosion rate since it gives an idea of how fast the metal dissolves in the corrosive media at the prevailing conditions. Hence, it can be used to determine the quality of various metallic structures after a given duration of adverse environmental impact. The OFAT-based method was applied, (varying one of the factors: inhibitor concentrations, temperature, and time, while the remaining two factors were maintained constant). In this method, 200 ml of blank 1 M H_2SO_4 was introduced into a 250 ml open beaker holding weighed mild steel coupons. Additionally, different inhibitor concentrations were then added to a 250 ml open beaker containing 200 ml of 1 M H_2SO_4. This process was performed for each mild steel coupon.

From time to time, variations in weight loss were observed at different concentrations of acid solution, at different temperatures between 303 K and 343 K; with and without the inhibitor concentrations of 0.2 g/L to 1.0 g/L. The coupons were removed, submerged in acetone, cleaned, and weighed again at regular intervals.

Experimental readings were recorded. Weight loss (Δw), corrosion rate (CR), inhibition efficiency (IE) and surface coverage (θ) were respectively determined with equations (1), (2), (3) and (4) **(**Umoren et al., 2021; Fouda et al, 2021; Onukwuli et al., 2024 (a, b), 2025).

$$\Delta w = w_i - w_f \quad (1)$$

$$CR = \frac{w_i - w_f}{At} \tag{2}$$

$$IE\% = \frac{\omega_0 - \omega_1}{\omega_0} * 100 \tag{3}$$

$$\theta = \frac{\omega_0 - \omega_1}{\omega_0} \tag{4}$$

Weight loss values in the inhibited and blank solution are symbolized by w_1 and w_0, respectively, while w_i and w_f signify the initial and final weights of mild-steel. 'A' symbolizes mild-steel total area, 't' is immersion time and θ, surface coverage.

2.2.4 Thermodynamic properties

Heat of adsorption was calculated with Equation (5).

$$Q_{ads} = 2.303R\left[\log\left(\frac{\theta_2}{1-\theta_2}\right) - \log\left(\frac{\theta_1}{1-\theta_1}\right)\right] * \frac{T_2 . T_1}{T_2 - T_1} \tag{5}$$

where R is the gas constant, and θ_1 and θ_2 are degrees of surface coverage at temperatures T_1 and T_2, respectively.

2.2.5 Fitting experimental data to isotherm models

The surface coverage data was utilized for the application of different isotherms, namely Langmuir (Equation 6), Frumkin (Equation 7), and Temkin (Equation 8) and Flory-Huggins (Equation 9) (Udeh et al., 2021; Umoren et al., 2021; Fouda et al., 2021; Onukwuli et al., 2024 (a, b), 2025**)**.

$$\text{Log}\left(\frac{C}{\theta}\right) = \log(C) - \log(K) \tag{6}$$

$$\log\left((C) * \left(\frac{\theta}{1-\theta}\right)\right) = 2.303 logK + 2\alpha\theta \tag{7}$$

$$\theta = -\frac{2.303 \log K}{2\,a} - \frac{2.303 \log C}{2\,a} \tag{8}$$

$$\log\left(\frac{\theta}{C}\right) = \log K + x log(1-\theta) \tag{9}$$

Gibb's free energy of adsorption (ΔG_{ads}) was calculated using Equation (10).

$$\Delta G_{ads} = -2.303RT log(55.5K) \tag{10}$$

2.2.6 Weight loss method using response surface methodology (RSM)

This was used in the experimental design of the weight-loss strategy. Temperature, time, and inhibitor concentration were the variables considered; the study's response was the efficiency of the expired drug. Accordance to earlier reports [Anadebe et al., 2019]**,** the response of each case was analyzed using RSM to further reveal the fitness of the model.

2.2.7 Prediction of inhibition efficiency using artificial neural network (ANN)

An input-output data problem was fitted using an ANN. It involved the selection of data with neural network fitting tool, which is followed by the creation of a network **(**Nnanwube and Onukwuli, 2020**).** As part of the process, the network was trained and its performance evaluated. The data were categorized into three: training, validation, and testing. The network was adjusted and validated to halt training when generalization stopped improving**.** It stopped when there was an increase in mean square error (MSE) of the validation samples. The MSE was measured as the average squared variance between the predicted outputs and actual targets. Lower values of MSE indicates a better model, as a zero value indicates no error. The statistical criterion was regression (R) values, which measured the relationship between the outputs and targets.

ANN optimization involving regression analyses, performance evaluations, and training analyses, were carried out using statistical tools, as shown in Equations (11), (12), and (13), respectively **(**Nnanwube and Onukwuli, 2020; Onukwuli et al., 2024 (a, b), 2025**).**

$$R^2 = 1 - \frac{\sum_{i=1}^{n}\left(Y_{exp,i} - Y_{pred.,i}\right)^2}{\sum_{i=1}^{n}\left(Y_{exp,i} - Y_{pred.,ave}\right)^2} \tag{11}$$

$$RMSE = \left(\frac{1}{n}\sum_{i=1}^{n}\left(Y_{pred} - Y_{exp}\right)^2\right)^{\frac{1}{2}} \tag{12}$$

$$SEP = \frac{RMSE}{Y_{exp,ave}} * 100 \tag{13}$$

where n is number of sample points, Y_{pred}, predicted efficiency, Y_{exp}, experimental efficiency, and $Y_{exp.\ ave}$, experimental average.

2.2.8 Mild-Steel (MS) Surface Study

MS samples were examined using the scanning electron microscope (SEM) (RhenomProx model).

2.2.9 Electrochemical Techniques

The effectiveness and type of expired drugs were determined using electrochemical techniques. Three electrodes that has electrochemical impedance spectroscopy (EIS) and potentiodynamic polarization (PDP) was used in the study. The reference, counter, and working electrodes were mild-steel specimens fixed in epoxy resin and exposed to the test solution. Electrochemical measurements were performed in accordance with the method previously reported (Omotioma et al., 2024a)**.**

3.0 Results and Discussion

3.1 Characteristics of Promethazine -Theoclate

3.1.1 Functional groups

The FTIR spectra of the drug are shown in Figure 1. Each spectrum shows the connection between the transmittance and wave number representing the functional groups. The identified functional groups are also presented in Table 1 and include O-H stretch, CO-NH-CO, C-H stretch, N-H deformation, C-O-C stretch, =C-H stretching and C-F stretch. The drug contained heteroatoms of nitrogen and oxygen.

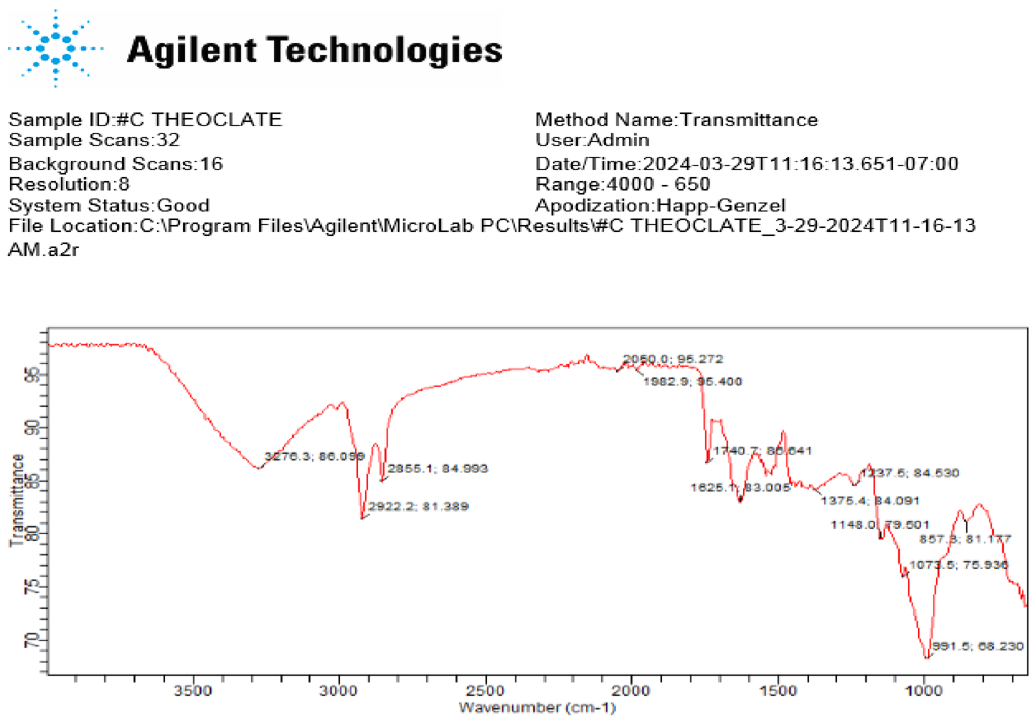

Figure 1: Infrared spectrum of the promethazine-theoclate

Table 1 lists peaks observed in spectroscopic analysis of promethazine-theoclate, their intensities, and corresponding functional groups and classes of compounds.

3.1.2 Chemical constituents of promethazine-theoclate

The chemical constituents of the drug as obtained by GC-MS analysis indicate that promethazine-theoclate contains phenol, 2,4-di-tert-butylphenol, tridecane, cyclo-hexadecane, n-Propyl 11-octadecenoate and 1-Heptadecene. The presence of these substances shows that promethazine-theoclate has the capacity to antagonize a variety of receptors, allowing it to be used for a number of applications including corrosion inhibition (Omotioma et al., 2024b).

3.2 Effects of Independent Factors

The effects of the process inhibitor of MS in H_2SO_4 solution are portrayed in Table 2. The weight loss and corrosion rate decreased with rise in inhibitor concentration. The efficiency also increased with concentration. Highest inhibition efficiency of 92.89 % (promethazine -theoclate) was reached at 0.8 g/L inhibitor concentration in 3 hours at 313 K because of increase in electrostatic attraction between molecules. Beyond the maximum point, the inhibition efficiency showed slight decrease. The observed retardation may be due to the force of attraction between the molecules of the inhibitor and surface of mild-steel [Paul et al., 2020]**.** Weight loss and corrosion rate increased with temperature. Consequently, an increase in temperature decreases the efficiency levels of promethazine-theoclate as an inhibitor. This may be due to the force of attraction of mild-steel **(**Paul et al., 2020; Deyab, 2020)**.**

The inhibition efficiency increased with time. It corroborates with the reports of previous research works [Onukwuli et al., 2021]**,** which stated that the efficiency of the inhibitor improves with time. The high inhibition efficiency may be due to viable hetero-atoms. The maximum inhibition efficiency recorded here (92.89 %) is higher than the value of 90.5 % obtained when furosemide drug was used as inhibitor for carbon steel corrosion in HCl media at a temperature of 318 K and inhibitor dosage of 300 ppm (Maksoud et al., 2024).

Table 1: Functional groups of promethazine-theoclate

S/N	Peaks	Intensity	Functional Group	Class of Compounds
1.	3276.3	86.099	O-H Strech	Carboxylic
2.	2922.2	81.389	C-H	Alkene and Alkyls
3.	2855.1	84.993	C-H	Alkene and Alkyls
4.	1982.9	95.400	C-H	Alkene and Alkyls
5.	1740.7	86.641	CO-NH-Co	Carbonyl Group
6.	1625.1	83.005	N-H Deformation	Carbonyl Group
7.	1375.4	84.091	C-O Stretching	Alcohols and Phenols
8.	1237.5	84.530	O-H Deformation	Alcohols and Phenols
9.	1148.0	79.501	C-O-C Stretch	Ethers
10.	1073.5	75.936	C-F Strech	Alkyl halides
11.	991.5	68.230	=C-H Stretching	Alkenes
12.	857.8	81.177	$=CH_2$ deformation	Alkene and Alkyls

The above details help to analyze the chemical structure and functional groups present in the compounds

Table 2: Effects of Independent Factors

Effect of time

Time (h)	ΔW_0 (g)	CR_0 (mg/cm^{2}h)	ΔW_1 (g)	CR_1 (mg/cm^{2}h)	IE (%)	Θ
1	0.157	17.44	0.028	3.111	82.17	0.8217
2	0.308	17.11	0.037	2.056	87.99	0.8799
3	0.506	18.74	0.036	1.333	92.89	0.9289
4	0.511	14.19	0.045	1.250	91.19	0.9119
5	0.527	11.71	0.051	1.133	90.32	0.9032
Effect of concentration (g/L)						
0.0	0.506	18.74				
0.2			0.175	6.481	65.42	0.6542

0.4			0.144	5.333	71.54	0.7154
0.6			0.103	3.815	79.64	0.7964
0.8			0.036	1.333	92.89	0.9289
1.0			0.048	1.778	90.51	0.9051
Effect of temperature (K)						
303	0.422	15.63	0.041	1.519	90.28	0.9028
313	0.506	18.74	0.036	1.333	92.89	0.9289
323	0.557	20.63	0.081	3.000	85.46	0.8546
333	0.722	26.74	0.147	5.444	79.64	0.7964
343	0.81	30	0.195	7.222	75.93	0.7593

3.3 Heat of adsorption

The heat of adsorption (Q_{ads}) for mitigating MS corrosion is portrayed in Table 3. Q_{ads} had negative values for all concentrations from 0.2 g/L to 1.0 g/L. This means that adsorption was accompanied by the release of heat. This was similar to the reports of Omotioma et al., (2024b**)**, where a negative value for the heat of adsorption was an indication of an exothermic process. The status of Q_{ads} showed flow of heat from the inhibitor to mild-steel interface at a seemingly higher temperature to the surroundings at a lower temperature.

Table 3: Heat of adsorption

Inhibitor Conc. (g/L)	0.2	0.4	0.6	0.8	1.0
Heat of adsorption, Q_{ads} (J/mol)	-56322.4	-57796.6	-73081	-67151.6	-53399.4

3.4 Adsorption Parameters Results

The results of these parameters are listed in Table 4. The Frumkin isotherm is the best-fitted isotherm. This assertion was based on the recorded highest average value of the coefficient of determination (R^2 average = 0.9885); which was closest to the critical value of 1 (one) compared to the average R^2 values of the other isotherms (Langmuir (0.9741), Temkin (0.8631) and Flory-Huggins (0.6206)). In the Temkin results, the attractive parameter (a) values were negative, implying no chemical reaction between mild steel and promethazine-theoclate. The lateral interaction term (α) at 313 K and 323 K were positive, from the Frumkin plot. This means there was a noticeable attraction between promethazine-theoclate and mild-steel surface. Positive values of size property (x) were revealed by analysis of the Flory-Huggins' isotherm, indicating reasonable layer of drug attachment to the mild-steel. Gibb's free energy was lower than -40.00 kJ/mol, hence adsorption mechanism was physical (Onukwuli et al., 2024(a, b), 2025)**.**

Table 4: Results of Adsorption parameters

Isotherms	Temp. (K)	R^2	K	ΔG_{ads} (J/mol)	Property	
Langmuir	313	0.9926	0.9192	-10218.7		
	323	0.9555	0.8297	-10219.3		
Temkin	313	0.8980	178.074	-10312.2	a	-2.8320
	323	0.8282	33.481	-10545.2		-2.1273
Frumkin	313	0.9942	0.02221	-10234.3	α	2.62365
	323	0.9768	0.0889	-10286.1		1.8540
Flory-Huggins	313	0.7028	4.4300	-10234.3	x	0.5998
	323	0.5383	2.4121	-10332.5		0.5245

3.5 RSM and ANN Results of Corrosion Control

The RSM and ANN results of corrosion control of mild steel using promethazine-theoclate are presented in Table 5. The experimental, RSM predicted and ANN predicted efficiencies are reported as functions of time, temperature and concentration. The maximum value of efficiency is 92.55 % at 0.8 g/L, 313 K and 3 hours, from the RSM analysis. This indicates that effects of the variables are parabolic and conform to the quadratic model.

Table 5: RSM and ANN values of promethazine-theoclate efficiency in H_2SO_4

Std	Runs	F A g/L	F B K	F C h	Actual IE (%)	RSM pred IE (%)	ANN pred IE (%)
4	1	1	323	1	60.76	60.84	60.74
3	2	0.6	323	1	46.67	47.2	46.65
13	3	0.8	313	1	84.03	82.64	84.01
15	4	0.8	313	3	92.55	93.03	92.53
20	5	0.8	313	3	92.55	93.03	92.53
12	6	0.8	323	3	77.59	77.05	77.57
1	7	0.6	303	1	59.86	61.21	59.84
8	8	1	323	5	75.69	74.7	75.67
5	9	0.6	303	5	62.78	63.06	62.76
16	10	0.8	313	3	92.55	93.03	92.53
18	11	0.8	313	3	92.55	93.03	92.53
9	12	0.6	313	3	77.58	74.5	77.56
14	13	0.8	313	5	90.54	90.5	90.52
6	14	1	303	5	77.75	77.58	77.73
19	15	0.8	313	3	92.55	93.03	92.53

2	16	1	303	1	68.86	68.3	68.84
17	17	0.8	313	3	92.55	93.03	92.53
11	18	0.8	303	3	86.38	85.49	86.36
10	19	1	313	3	86.93	88.58	86.91
7	20	0.6	323	5	52.71	53.63	52.69

F A = inhibitor concentration, F B = temperature, F C = time.

3.5.1 Quadratic models' ANOVA

The ANOVA of the quadratic model for the promethazine-theoclate efficiency in H_2SO_4 solution is shown in Table 6.

Table 6: Quadratic models' ANOVA for promethazine-theoclate efficiency in H_2SO_4 solution

Source	Sum of Sq	Df	Mean Sq	F-value	p-value	
Model	4160.60	9	462.29	220.43	< 0.0001	Sig
A	495.48	1	495.48	236.26	< 0.0001	
B	178.17	1	178.17	84.96	< 0.0001	
C	154.37	1	154.37	73.61	< 0.0001	
AB	21.45	1	21.45	10.23	0.0095	
AC	27.60	1	27.60	13.16	0.0046	
BC	10.49	1	10.49	5.00	0.0493	
A^2	363.14	1	363.14	173.16	< 0.0001	
B^2	380.41	1	380.41	181.39	< 0.0001	
C^2	114.81	1	114.81	54.75	< 0.0001	
Residual	20.97	10	2.10			
Lack of Fit	20.97	5	4.19			
Pure Error	0.0000	5	0.0000			
Cor Total	4181.57	19				
Std. Dev.	1.45		R^2		0.9950	
Mean	78.17		Adj R^2		0.9905	
C.V. %	1.85		Pred R^2		0.9611	
			Adeq Precision		44.7538	

3.5.2 Quadratic model of inhibition efficiency of Promethazine -Theoclate

The generated models are quadratic. The coded equation was useful in detecting the comparative effect of the variables (factors) by comparison of the coefficients. The equation of actual factors is not to be applied to evaluate relative effect of each variable since the coefficients were scaled to incorporate the units of each variable and the intercept was not situated at the middle of the design space.

Equation in terms of coded factors for promethazine-theoclate in H_2SO_4 is presented as Equation (14).

$$\text{Inhibitor efficiency} = +93.03+7.04A-4.22B+3.93C+1.64AB+1.86AC+1.15BC-11.49A^2-11.76B^2-6.46C^2 \quad (14)$$

Equation in terms of actual factors for promethazine-theoclate in H_2SO_4 is presented as Equation (15).

Inhibitor efficiency = -11259.87613 + 224.64955Inhibitor concentration + 72.37729Temperature - 9.97770Time + 0.818750Inhibitor concentration x Temperature + 4.64375Inhibitor concentration * Time + 0.057250Temperature x Time - 287.28409Inhibitor concentration^2 - 0.117614Temperature^2 - 1.61534Time^2 (15)

A graphical analysis of the predicted versus actual inhibition efficiencies of the drug is presented in Figure 2. This is a linear graph, with points close to the line of the best fit. This figure also shows the generated data.

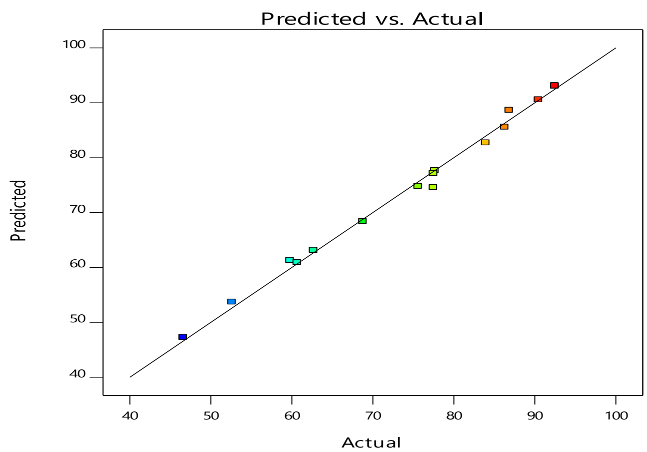

Figure 2: Predicted against actual efficiency of promethazine-theoclate in H_2SO_4

3.5.3 Three dimensional (3-D) plots of promethazine-theoclate

The 3-D plots of RSM analysis of the efficiencies of the inhibitor are presented in Figure 3 (a-c). The interactive influence of the independent factors on the dependent factor displayed parabolic curves in all cases. The nature of the graphs (parabolic curves) supports the earlier explanation that the quadratic model fits the factors. In addition, the 3-D plots showcased optimum parameters as determined by the optimization tool.

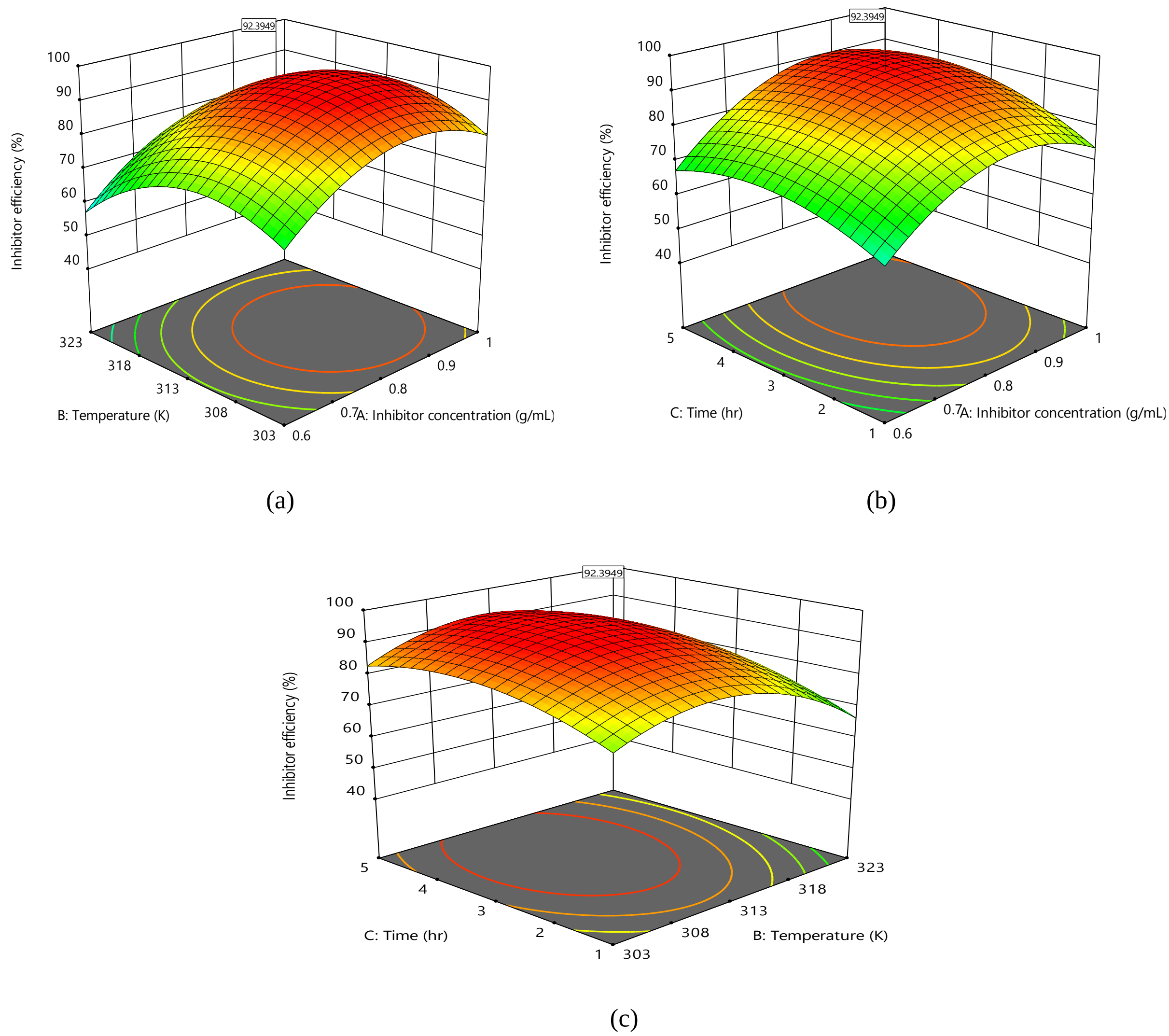

Figure 3: Efficiency versus (a) temperature and concentration (b) time and concentration (c) time and temperature of promethazine-theoclate in H_2SO_4.

3.5.4 Optimum results of RSM

The optimum values of the corrosion control parameters are presented in Table 7. In H_2SO_4 solution, promethazine-theoclate had higher efficiency of 92.39%. This may be due to the higher quality of the phytochemicals and the intensity of the functional groups. The recorded high efficiencies show that promethazine-theoclate is suitable for controlling mild-steel corrosion in acid solutions.

Table 7: Optimum results of the corrosion inhibition process

Media	Opt. inh. conc. (g/L)	Opt. temp. (K)	Opt. time (h)	Opt. IE (%)
Mild steel in H_2SO_4 with Promethazine - Theoclate	0.85	316.16	3.46	92.39

3.5.5 Validation of results

Table 8 presents the validation of the RSM results. At optimum conditions, the predicted and experimental values of the inhibition efficiency were compared using the percentage deviation as a statistical tool. Recorded IE values had less than 5 % deviation. Hence, the model effectively predicted the results obtained from the experiment.

Table 8: Validation of results

Media	Opt. conc. (g/L)	Opt. temp. (K)	Opt. time (h)	Opt. IE (%)	Exp. IE (%)	Percentage deviation (%)
Mild steel in H_2SO_4 with promethazine-theoclate	0.85	316.16	3.46	92.39	92.23	0.16

3.6 ANN plots

The ANN results for corrosion control are presented using the regression evaluation graphs in Figure 4. Validation and testing were performed on the graphical results. Points of the training data were clustered on the line of the best fit. Statistical analysis of the performance in terms of the mean square error and coefficient of determination are equally presented.

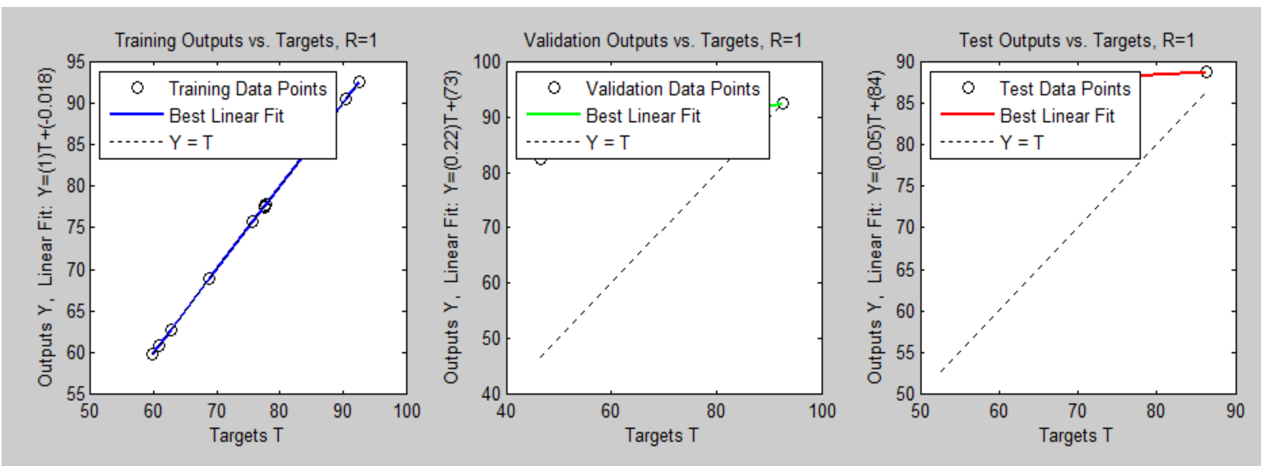

(a) (b) (c)

Figure 4: ANN regression for prediction of efficiency of promethazine-theoclate: (a) training output, (b) validation output, (c) test output

3.7 Comparison of ANN and RSM results

The comparative results of the ANN and RSM in terms of RMSE, SEP, and R^2 are presented in Table 9. ANN had a smaller RMSE and SEP. This observation showed a better prediction than RSM, which agrees with previous studies **(**Nnanwube and Onukwuli, 2020; Omotioma et al., 2024b**),** where the superiority of ANN over RSM was mentioned. Based on the coefficient of determination (R^2), the ANN also had a higher value. Thus, ANN gave better performance than RSM in predicting the efficiency of promethazine-theoclate as an inhibitor.

Table 9: Comparison of predictions of ANN and RSM in terms of RMSE, SEP and R^2

Comparison of Prediction	RMSE	SEP	R^2
RSM	1.023863	1.309765	0.985884
ANN	0.0180	0.023026	0.999996

3.8 SEM-EDX results

The SEM-EDX results are presented in Figures 5a and 5b, where the surface morphologies of mild-steel, were subjected to corrosion in uninhibited and inhibited H_2SO_4 solution. The mild-steel in Figure 5a (i and ii) in the uninhibited solution was deeply corroded compared with the inhibited solutions in Figure 5b (i and ii), which had a lesser corrosion impact. The observations made in this study are in line with the reports of Onukwuli et al. (2025), which stated that metal was more seriously damaged in an uninhibited medium than in an inhibited medium. The results show changes in the elemental compositions of mild-steel surface. The effective corrosion inhibition of mild-steel in acid solutions using promethazine-theoclate was established by surface morphological results.

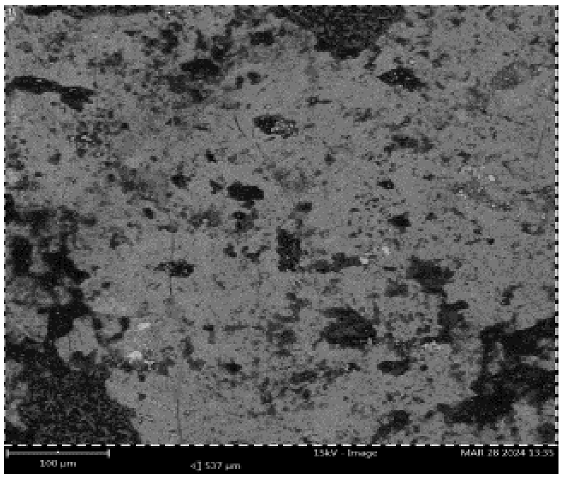

ai

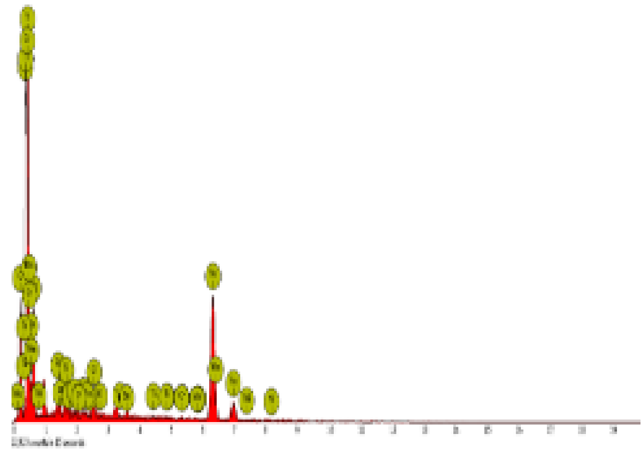

aii

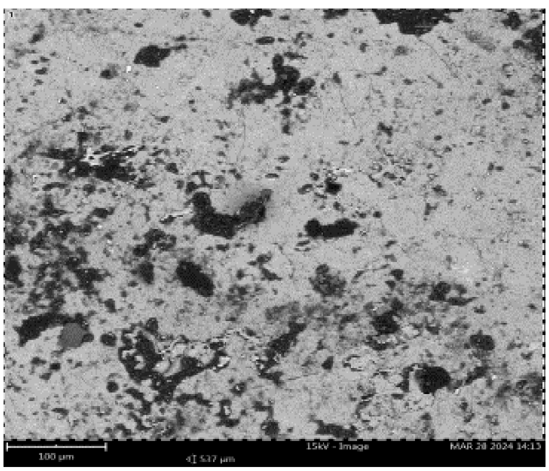

bi

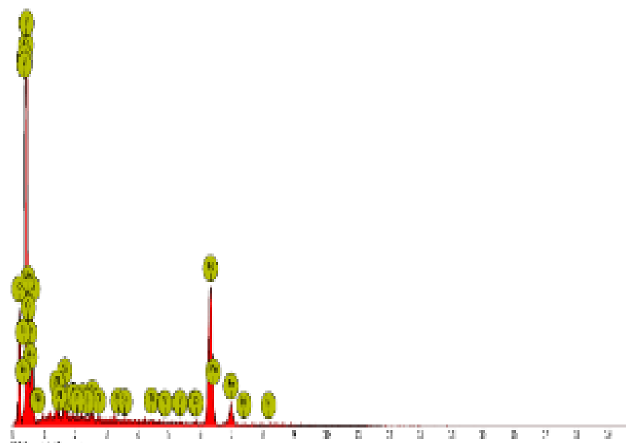

bii

Figure 5: SEM-EDX result of promethazine theoclate (a) (i and ii) in an uninhibited H_2SO_4 (b) (i and ii) in inhibited H_2SO_4

The mild-steel in Figure 5a has the following elements with their numbers, symbols, atomic concentrations and weight concentrations in the order of Iron (Fe) 26, 24.06 and 55.29; Carbon (C) 6, 69.35 and 34.28; Silicon (Si) 14, 1.50 and 1.73; Chlorine (Cl) 17, 1.41 and 2.06; Aluminum (Al) 13, 2.02 and 2.25; Tin (Sn) 50, 0.21 and 1.02; Manganese (Mn) 0.10, 0.23 and 0.66; Sulfur (S) 16, 0.30 and 0.33; Titanium Ti 22, 0.15 and 0.25; Phosphorus P 15, 0.35 and 0.45; Vanadium V 23, 0.21 and 0.41; Nickel Ni 28, 0.00 and 0.00; and Chromium Cr 24, 0.13 and 0.29. Similarly, in Figure 5b, the mild-steel had the following elements: Iron (Fe) 26, 28.11 and 61.54; Carbon (C) 6, 66.92 and 31.51; Silicon (Si) 14, 1.73 and 1.91; Aluminum (Al) 13, 2.02 and 2.25; Tin (Sn) 50, 0.15 and 0.71; Chlorine (Cl) 17, 0.54 and 0.75;

Sulfur S 16, 0.29 and 0.36; Phosphorus P 15, 0.29 and 0.33; Nickel Ni 28, 0.00 and 0.00; Chromium Cr 24, 0.16 and 0.33; Vanadium V 23, 0.06 and 0.12; Titanium Ti 22, 0.27 and 0.51; and Manganese Mn 25, 0.29 and 0.35.

3.9 Electrochemical Results

The electrochemical results presented in Figures 6a and 6b, are for potentiodynamic polarization (PDP) and electrochemical impedance spectroscopy (EIS), respectively. Increased inhibitor concentration inhibited cathodic and anodic reactions as observed from polarization curves displayed in Figure 6a (PDP plots), indicating that promethazine-theoclate was a mixed-type inhibitor. Higher inhibitor concentrations produced larger capacitive loops in inhibited solution as shown in Figure 6b (EIS plots), with 0.8 g/L of the inhibitor producing the highest loop. The result indicates that the mild-steel had a higher resistance to corrosion in the inhibited solution, with 0.8 g/L as the optimum concentration. EIS technique results also indicate a charge-transfer process-controlled corrosion reaction**.**

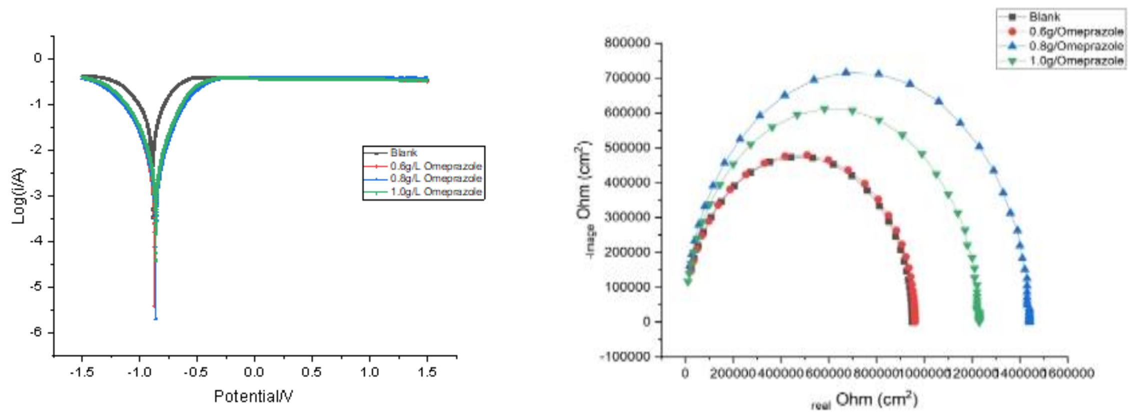

(a) PDP (b) EIS

Figure 6: Electrochemical results in blank and inhibited H_2SO_4 solution (a) PDP (b) EIS

4.0 Conclusion

This work investigated the inhibition properties of promethazine-theoclate as an inhibitor for MS corrosion in H_2SO_4 media. The main functional groups of the drug are O-H stretch, CO-NH-CO, C-H stretch, N-H deformation, C-O-C stretch, =C-H stretching and C-F stretch. The drug contained nitrogen and oxygen heteroatoms. The Frumkin isotherm was the best fitted isotherm, with Gibb's free energy values of -10.23 kJ/mol and -10.29 kJ/mol at 313 K and 323 K, respectively. Hence, adsorption of the inhibitors' molecules was physical, not chemisorption. The gravimetric analysis carried out gave maximum inhibition efficiency of 92.89 %. Quadratic model adequately described relationships between efficiency and the inhibitor factors and optimum efficiency of 92.39% was achieved via RSM optimization, indicating a correlation between the experimental and optimization results. ANN gave improved prediction of the inhibition efficiency when compared with the RSM. From the results of EIS, charge-transfer characterized the corrosion process. Promethazine-theoclate was seen as mixed-type inhibitor in corrosive media and can be applied to inhibit MS corrosion. Hence this study has established the possibility of using expired pharmaceutical in industrial corrosion control.

References

Anadebe, V. C., Onukwuli, O. D., Omotioma, M., Okafor, N. A., 2019. Experimental theoretical modeling and optimization of inhibition efficiency of pigeon pea leaf extract as anti-corrosion agent of mild steel in acid environment. Material Chemistry and Physics, 233, 120-132.

Deyab, M. A., 2020. Understanding the anti-corrosion mechanism and performance of ionic liquids in desalination, petroleum, pickling, de-scaling, and acid cleaning applications. Journal of Molecular Liquids, 309(1), 113107–113139.

Fouda, A. S., Ahmed, A. M., El-Darier, S. M., Ibrahim, I. M., 2021. Wihanias omnifera extract as a friendly corrosion inhibitor of carbon steel in HCl solution. International Journal of Corrosion and Scale Inhibition, 10(1), 245–261.

Maksoud, S. A. E., Fouda, A. E. A., Badawy, H., 2024. Furosemide drug as a corrosion inhibitor for carbon steel in 1.0 M hydrochloric acid. Sci Rep., 14, 9052. https://doi.org/10.1038/s41598-024-58713-4

Nnanwube, I. A., Onukwuli, O. D., 2020. Modeling and optimization of galena dissolution in a binary solution of nitric acid and ferric chloride using artificial neural network coupled with genetic algorithm and response surface methodology, South African Journal of Chemical Engineering, 32, 68-77.

Omotioma, M., Onukwuli, O. D., Nnanwube, I. A., 2024a. Testing the inhibition efficiency of the castor oil leaf as corrosion inhibitor of mild steel in H_2SO_4. Heliyon, 10, e31168. https://doi.org/10.1016/j.heliyon.2024.e31168

Omotioma, M., Okolo, N. W., Okorie, O., Ekete, J. A., Aliozo, O. S., 2024b. Corrosion control of mild steel in hydrochloric acid solution using extract of sweet potato leaf as green inhibitor. World Scientific News, (189), 23-37.

Omotioma, M., Onukwuli, O. D., 2019. Phytochemical and thermodynamic studies of pawpaw leaf (Asimina trilola) extract as corrosion inhibitor of zinc in KOH medium. Journal of the Nigerian Society of Chemical Engineers, 34(1), 53-61.

Omotioma, M., Onukwuli, O. D., Obiora-Okafo, I., 2019. Phytochemicals and inhibitive properties of cashew extract as corrosion inhibitor of aluminum in H_2SO_4 medium. Latin American Applied Research, 49, 99-103.

Onukwuli, O. D., Udeh, B. C., Omotioma, M., Nnanwube, I. A., 2021. Corrosion inhibition of aluminum in hydrochloric acid medium using cimetidine as inhibitor: Empirical and optimization studies, Anti-corrosion methods and materials, 68(5), 385-395.

Onukwuli, O. D, Omotioma, M., 2019. Study of bitter leaves extract as inhibitive agent in HCl medium for the treatment of mild steel through pickling, Portuagaliae Electrochemical Acta, 37 (2), 115-121.

Onukwuli, O. D., Nnanwube, I. A., Ochili, F. O., Omotioma, M., 2024a. DFT, Experimental and Optimization Studies on the Corrosion Inhibition of Aluminium in H_2SO_4 with Danacid as Inhibitor. Results in Engineering, 24, 103113. https://doi.org/10.1016/j.rineng.2024.103113

Onukwuli, O. D., Nnanwube, I. A., Ochili, F. O., Obibuenyi, J. I., 2024b. Assessing the efficiency of danacid as corrosion inhibitor for aluminium in HCl medium: Experimental, theoretical and optimization studies, Heliyon, 10, e40994. https://doi.org/10.1016/j.heliyon.2024.e40994

Onukwuli, O. D., Nnanwube, I. A., Ochili, F. O., Omotioma, M., Obibuenyi, J. I., 2025. Corrosion inhibition effects of eco-friendly clarithromycin molecules on aluminium in hydrochloric acid solution via experimental, theoretical and optimization approach. Results in Chemistry, 13, 101987. https://doi.org/10.1016/j.rechem.2024.101987

Paul, P. K., Yadav, M., Obot, I. B., 2020. Investigation on corrosion protection behaviour and adsorption of carbon-hydrazide-pyrazole compounds on mild steel in 15% HCl solution: Electrochemical and computational approach. Journal of Molecular Liquids, 314, 11313.

Udeh, B. C., Onukwuli, O. D., Omotioma, M., 2021. Application of metronidazole drug as corrosion inhibitor of mild steel in hydrochloric acid medium. Journal of Engineering and Applied Sciences, 18(1), 329-347.

Umoren, S. A., Eduok, U. M., Solomon, M. M., Udoh, A. P., 2021. Corrosion inhibition by leaves and stem extracts of Sida acuta for mild steel in 1M H_2SO_4 solutions investigated by chemical and spectroscopic techniques. Arab. J Chem., 9, 209-224.